Research Article

Composite concrete beam with multi-web cold-formed steel section

Ahmed Youssef Kamal * [ID], Nader Nabih Khalil [ID]

Department of Civil Engineering, Benha University, Benha, Egypt

ABSTRACT

Lately, structural engineers use cold-formed steel sections (CFS) in buildings due to its light-weight and easy shaping. Encasing the cold-formed steel sections by concrete avoiding the structure elements some of its disadvantages especially buckling. This paper reports an experimental test program for beams with a multi-web cold-formed steel section encased by reinforced concrete. Eleven (full-scale) specimens have tested under mid-span concentrated load, the experimental test program designed to cover many cold-formed steel section variables such as (web number, web height, and the steel section length). Comparison between the experimental results for specimens with encased steel cold-formed section and that for reference beam have presented. The experimental results show that the cold-formed steel webs number has a noticeable influence on the structural behaviour of the beam, such as increasing the beam load capacity. The beam load capacity, failure mode and the beam ductility have analysed, and some preparatory criteria for a sufficient outline have presented.

1. Introduction

Cold-formed steel members have broadly used as a part of the structural building because of their high strength-weight ratio, and for their ease and low-cost of manufacture. Yu (2010) has summarized the commonly used cold-formed steel section shapes for different applications. United States manufacturing associations introduced catalogs for the cold-formed steel (CFS) shapes, such as that provided by the Steel Framing Industry Association (SFIA) (2012). Cold forming technology restricts the cold-formed steel members' thickness in a range between 0.8 and 3 mm, Hancock (2007).

The buckling of the element cross-section under compression or shear may occur before the overall member failure; this phenomenon called local buckling. Thus, the CFS local buckling becomes a hindrance to the extensive use of thin-walled sections. Modifying the CFS cross-sections shape can significantly enhance the structure member load capacity and overcome the problem of local buckling in addition to reducing costs compared to the commonly used shapes "U-section, C-section, etc." However, previous researchers, focused on solutions

leading to cross-sections that cannot be effectively manufactured by the current cold-forming processes (Gilbert et al., 2012a, 2012b; Wang et al., 2016; Liu et al., 2004; Madeira et al., 2015; Leng et al., 2011; Moharrami et al., 2014). Pham et al. (2014) have reported that providing a longitudinal web stiffener in the direction of the longitudinal stresses reduces the web local buckling. Ye et al. (2016) said that, adding intermediate web stiffeners to plain CFS channel cross-sections provided minimum effect on the element flexural capacity. Most of previous studies on the cold-formed steel section members focused on the buckling of the members when they loaded by axial and bending loads. Lanc et al. (2015) have applied Bernoulli beam theory for bending, and Vlasov theory for beam torsion to illustrate the buckling behavior of thin-walled functionally graded sandwich box beam. A new analytical expression for computing web shear buckling of box sections was introduced by Bedair (2015), considering the flange restraints. Analytical formulas have developed to evaluate the global and local buckling strengths, to obtain solutions in a design constrained by geometric conditions. The results of their study indicated better flexural performance compared

to the traditional lipped or plain channel sections. Ma et al. (2015), have optimized the CFS compression and bending members with respect to their capacity according to EC3 (2005).

Compared with traditional reinforced concrete structure, the encased beam has a higher bearing capacity and ductility. Besides, it is also an economic structure element and easily constructed compared to load capacity gained. Because of these characteristics, it is widely used in constructions such as high-rise buildings and bridges. The modern building has a higher demand for the construction height and span length. Encased beam, which takes the advantage of both concrete and cold-formed steel (CFS) members can raise the element load capacity and decrease the weight of the structure. Ammar et al. (2012), said that the high percentage of the steel area in encased beam improves the beam ductility. Based on the previous literature review the beneficial effect of using the CFS is obvious, in our paper, we aimed that encasing the cold-formed steel (CFS) members in concrete will restrict the local buckling of cold-formed steel section. In addition, providing multi-web section will decrease the web slenderness ratio, which has the direct effect to overcome the local buckling problem.

2. Material Properties

Eleven specimens were prepared and tested in Benha Concrete Laboratory, Benha Faculty of Engineering, Egypt. One of them was concrete beam reinforced by only upper and lower steel bars referred as reference beam. Ten specimens were enhanced by multi-web cold-formed section; with the same reference beam concrete dimensions.

All specimens were with full-scale beams loaded by mid-span concentrated load. All beam specimens had a square concrete cross-section with side length of 150 mm. The total concrete specimen length and the clear length are identical for all specimens, with 1500 mm and 1400 mm respectively, as shown in Fig. 1.

All specimens were reinforced by two bars with 12 mm diameter upper and lower (high tensile steel) as a tension and compression reinforcement, equivalent to reinforcement ratio of 0.02, with average yield strength of 37 kg/mm². The average elastic modulus for all reinforcements was 20900 kg/mm². For shear resistance, closed mild steel stirrups with 8 mm diameter were provided and equally distributed with space of 200 mm (center to center) along the specimen length; stirrups existence makes a good engagement to the longitudinal bars, and enhances the beam ductility, as shown in Fig. 2. The concrete cover was taken as 10 mm all over the beam section. The average laboratory concrete compressive strength was 3.1 kg/mm², with average concrete volume weight of 2.3 kg/cm³; as a result of laboratory tests.

Table 1 shows the details of the experimental program, to evaluate and monitoring the studied parameters effect on the structural behavior of the encased beams using multi-web cold-formed steel sections. Specimens were divided into three groups with three variables, first group with different numbers of webs, the second group with variable web normalized height (η) (which defined as the cold-formed steel members height divided by the concrete section height) and the third one with variable cold-formed steel sections normalized length (λ) (which defined as the cold-formed steel members length divided by the concrete section length).
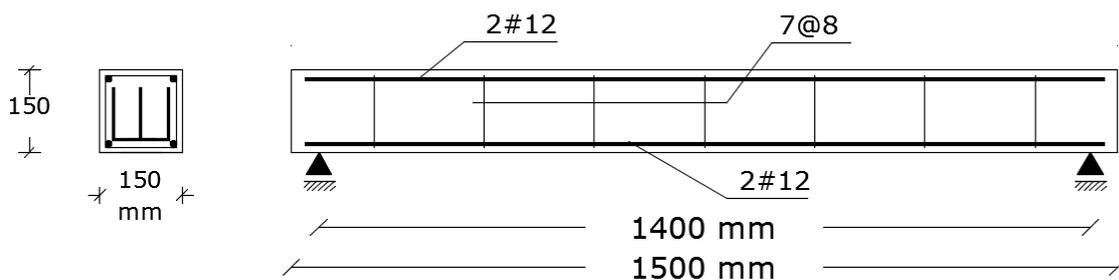
Fig. 1. Specimen dimensions.

Fig. 2. Upper and lower specimen reinforcement.

Table 1. Specimen details.

| | Specimen Code* | Cold-formed steel section | | | | Normalized height ($\eta = h_s/h$) | Normalized height ($\lambda = L_s/L$) |
		h_s (mm)	b_s (mm)	L_s (mm)	Web Number		
Group A	MWS1-1	---	110	1450	---	0	1
	MWS1-2	95	110	1450	1	0.63	1
	MWS1-3	95	110	1450	2	0.63	1
	MWS1-4	95	110	1450	3	0.63	1
	MWS1-5	95	110	1450	4	0.63	1
	MWS1-6	95	110	1450	5	0.63	1
Group B	MWS2-1	---	110	1450	---	0	1
	MWS2-2	50	110	1450	3	0.33	1
	MWS2-3	70	110	1450	3	0.47	1
	MWS2-4	95	110	1450	3	0.63	1
Group C	MWS3-1	95	110	460	3	0.63	0.33
	MWS3-2	95	110	930	3	0.63	0.66
	MWS3-3	95	110	1450	3	0.63	1
* MWSx-x: Multi-Web Section (Group number-Specimen number)							

Ten specimens were divided to three groups, (MWS1, MWS2 and MWS3), with different number of web (0, 1, 2, 3, 4 and 5) equally spaced web, different web height of (0, 50, 70 and 95 mm), and different (CFS) length (460, 930, and 1450 mm), as shown in Figs. 3(a-c). All the cold-formed steel section (CFS) was with constant thickness of 2 mm, and average yield strength of 28 kg /mm². The centroids of both the cold-formed steel section and the concrete specimen cross section were vertically coincident.

(a) Group A

3. Test Setup

As shown in Fig. 4, specimens were simply supported by two concrete blocks on a loading frame. All specimens were loaded by mid-span vertical load, applied by a 100 t hydraulic jack capacity connected to digital recording apparatus. Vertical displacements were recorded by Linear Variable Differential Transformer (LVDT's) with magnetic base, distributed along the specimen length. The (LVDT's) were distributed as two in the right side of the specimen (LVDT 1, 2), one under the concentrated load (LVDT 3) and one at mid-span between the applied concentrated load and the left support (LVDT 4), as shown in Fig. 4.

To measure the longitudinal strain at the mid-span of the specimen, strain gauge with a length of 10 mm were pasted on the (CFS) mid-span, and covered by water-proof material, as shown in Fig. 5. All results (load, vertical deflections, and strain) were automatically recorded by a computer system and saved as Excel file format.
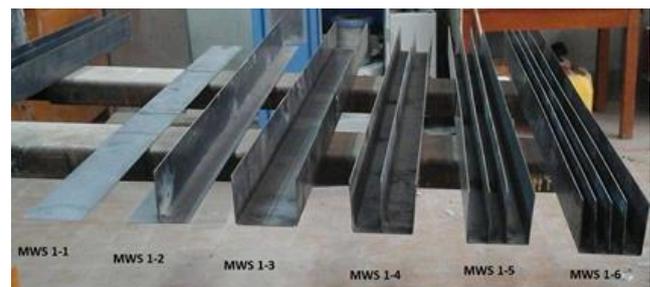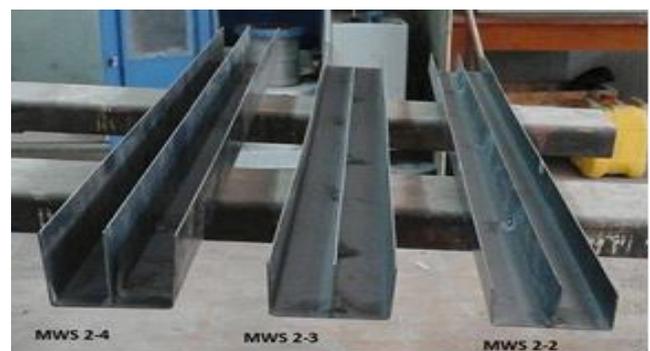
(b) Group B

(c) Group C

Fig. 3. Groups details.
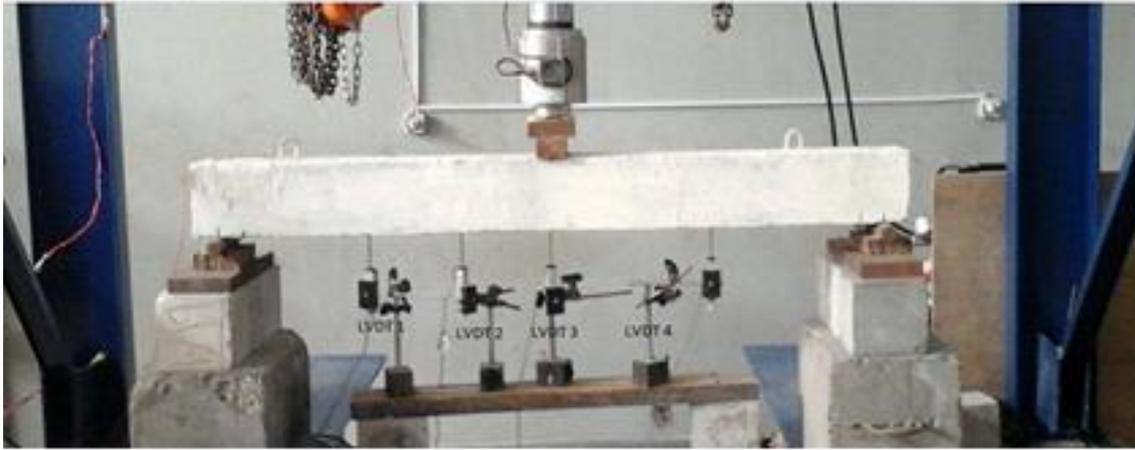
Fig. 4. The linear variable differential transformer distribution.

Fig. 5. Mid-span strain gauge.

4. Results and Discussion

4.1. Cracking and failure load

The reference beam specimen failed in ductile flexure mode, with a beam load capacity (P_f=4100 kg), and with cracking load (P_{cr}=2700 kg), Table 2. According to the observation for the reference beam, flexure concrete first cracks initiated at 66% of the beam load capacity at the bottom zone and extended up to about 85% of the beam height, followed by the first diagonal crack at about 92% of the beam load capacity. All cracks grew in size and number toward the applied load until failure, as shown in Fig. 6.

Fig. 7 represented the first cracking initiation load and the failure load as a percentage of that of reference beam (normalized load).

Table 2. Specimens' failure mode and ductility.

Specimen Code	Cracking load P_{cr} (kg)	Failure load P_f (kg)	Cracking factor ($F_{cr} = P_{cr}/P_f$) (%)	Mode of failure	Deflection at first crack Δ_{cr} (mm)	Deflection at failure Δ_f (mm)	Factor of ductility F_d
MWS1-1	1840	2425	76	Flexural / Splitting	2.10	42.19	15.2
MWS1-2	2040	3210	64	Flexural / Splitting	3.17	43.73	13.8
MWS1-3	2855	4275	67	Local buckling	2.7	33.03	9.7
MWS1-4	3300	4330	76	Flexural / Local buckling	4.07	19.24	4.72
MWS1-5	3370	4780	70	Flexural / Local buckling	4.66	20.56	4.41
MWS1-6	3160	5400	59	Support bearing failure	4.32	11.95	2.77
MWS2-1	1840	2425	76	Flexural / Splitting	2.10	42.19	15.2
MWS2-2	2500	3220	78	Flexural / Local buckling	4.07	32.76	8.05
MWS2-3	2250	2800	80	Local buckling	3.45	34.2	9.91
MWS2-4	3300	4330	76	Flexural / Local buckling	4.07	19.24	4.72
MWS3-1	2960	4800	62	Flexural / Shear	5.02	23.14	4.61
MWS3-2	3160	4800	66	Flexural / Shear	4.15	15.42	3.72
MWS3-3	3300	4330	76	Flexural / Local buckling	4.07	19.24	4.72
Reference beam	2700	4110	66	Flexural	4.8	31.2	6.5

Fig. 6. Reference beam crack pattern.
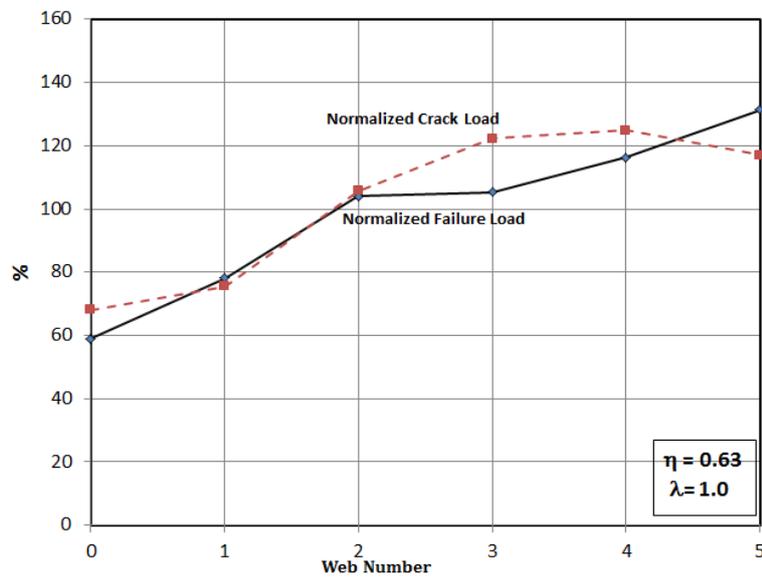
(a) Group A
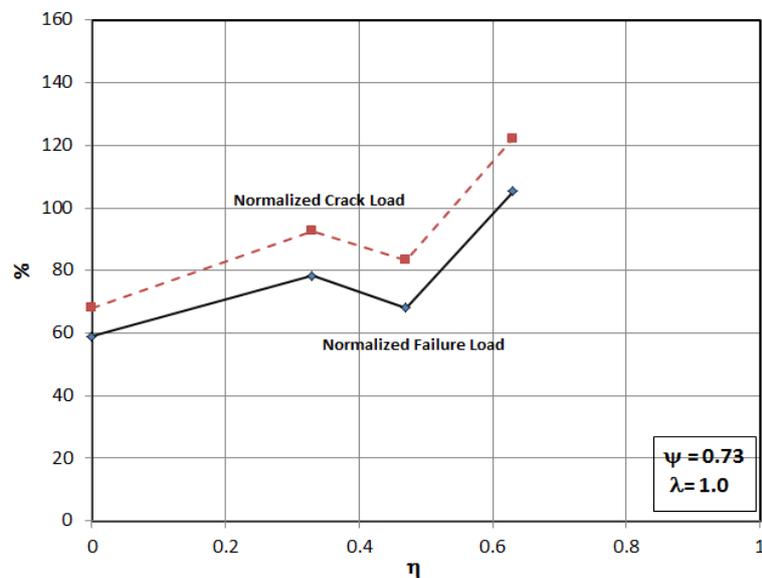
(b) Group B

Fig. 7. (continued)

(c) Group C
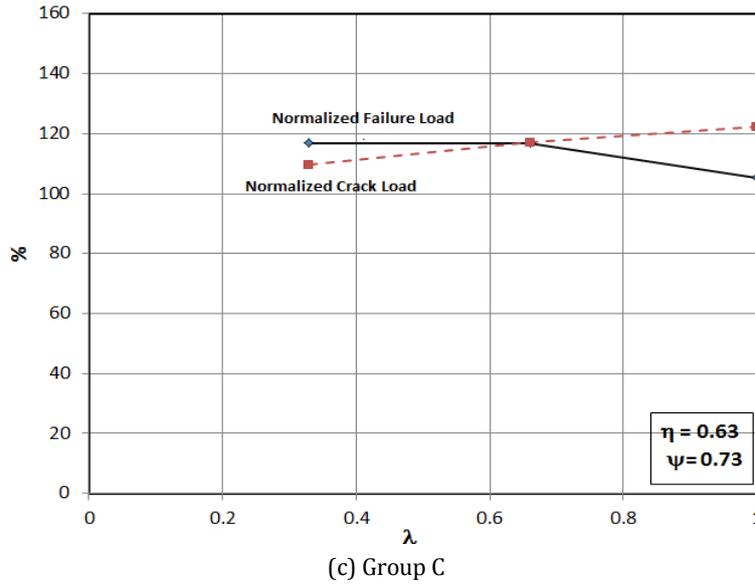
Fig. 7. Normalized crack and failure loads.

Providing the multi-web sections (MWS) with (ψ=0.73, η=0.63, λ=1.0), (ψ defined as the cold-formed steel members width divided by the concrete section width) and with different number of web (MWS1-3, MWS1-4 and MWS1-5), increase the beam load capacity by (4, 5, and 16% respectively) compared with the reference beam. Those models shared in similar failure mode, initiation of bottom flexure concrete cracks followed by concrete side crashing due to local buckling occurred in the (CFS) web; as a result of relatively small concrete cover resist the (CFS) web local buckling, as shown in Figs. 8(c-e). While shear splitting failure led the models with no web and one centered web (MWS1-1, MWS1-2) to fail with a load capacity less than the reference beam by (41, 22% respectively), as shown in Figs. 8(a-b). Sudden failure (without noticeable concrete flexure cracks

observation), due to support bearing failure was observed for model (MWS1-6), with noticeable increase of 31% in the beam load capacity compared with the reference beam, as shown in Fig. 8(f). Multi-web sections in models (MWS1-3, MWS1-4, MWS1-5, & MWS1-6) delayed the initiation of concrete cracks by (6, 22, 25, and 17%) respectively, with respect to that of reference beam, while for models (MWS1-1, MWS1-2) the concrete cracks initiated early by (32, 24%) respectively, than of that in reference beam, as shown in Fig. 7(a).

Average decreasing by (25, 35% in average) in the mid-span strain was recorded for models (MWS1-5 and MWS1-6) compared with model with one centered web. Beam with no web and one centered web cold-formed steel section fail before the cold-formed section reach yield, as shown in Fig. 9.

(a) MWS1-1

(b) MWS1-2

Fig. 8. (continued)

(c) MWS1-3

(d) MWS1-4

(e) MWS1-5
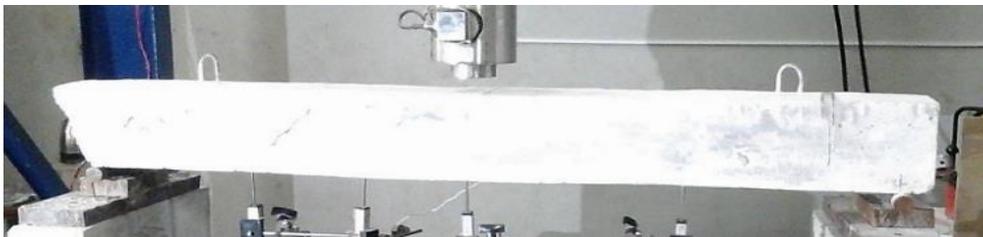
(f) MWS1-6

Fig. 8. Failure mode for models (group A).
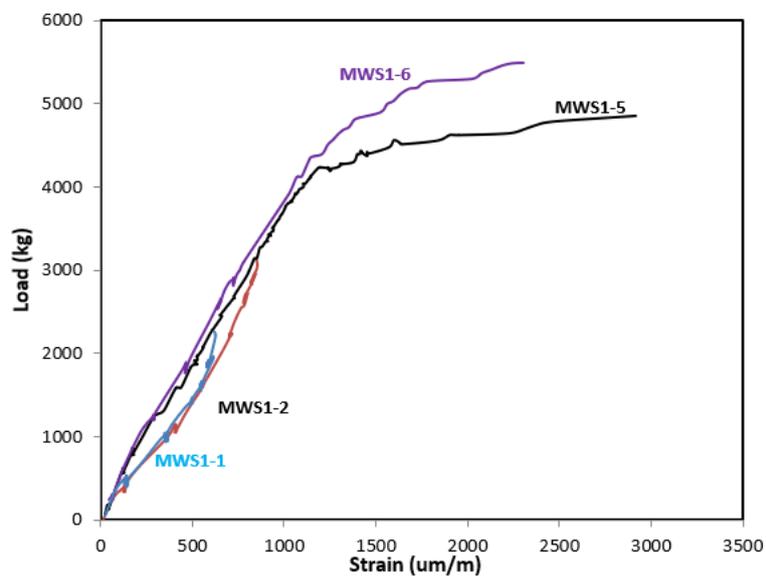
Fig. 9. Mid-span strain (Group A).

Web local buckling of models with three-web section, constant normalized width and length (ψ=0.73, λ=1.0), and with variable normalized height (η), led the models (MWS2-2, MWS2-3) to fail early, with decreasing in the load capacity by (22, 32% respectively), compared with the reference beam, as shown in Figs. 10(b-c). While shear-splitting failure led the model (MWS2-1) to fail with a decreasing percentage of 41%, in beam load capacity with respect to the reference beam, as shown in Fig. 10(a). Model (MWS2-4) with three-web section (η=0.63, ψ=0.73, λ=1.0) recorded a little increase by 5% in the load capacity compared with the reference beam with local buckling failure, as shown in Fig. 10(d). As Models (MWS2-1, MWS2-2 and MWS2-3) reached failure load early than reference beam, the concrete cracks initiation for those models were initiated early by (22, 8 and 17%) respectively, compared with the reference beam. While the concrete cracks initiation for model (MWS2-4) delayed by 22% than that of reference beam, as shown in Fig. 7(b).
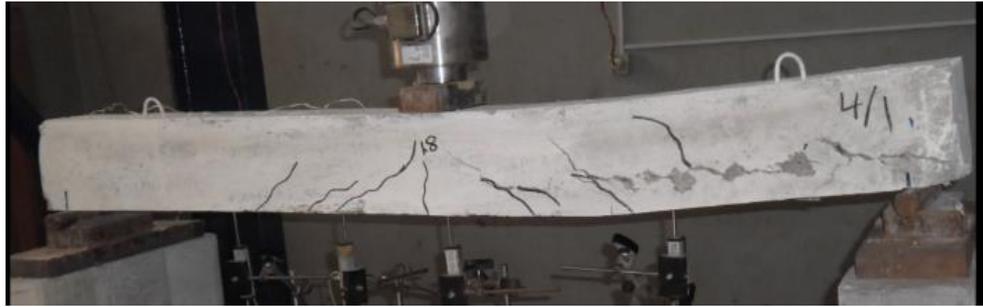
(a) MWS2-1
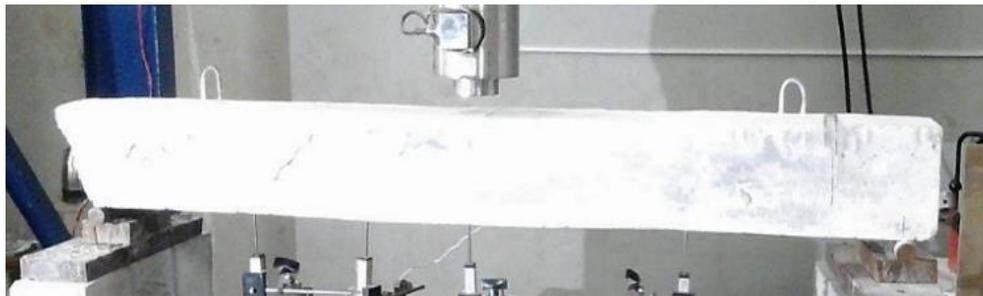
(b) MWS2-2

(c) MWS2-3

(d) MWS2-4

Fig. 10. Failure mode for models (group B).

Providing the three-web cold-formed steel section (η=0.63, ψ=0.73), with different values of normalized length (MWS3-1, MWS3-2 and MWS3-3) increase the beam load capacity by (17, 17, and 5%, respectively), compared with the reference beam. Decreasing the three-web cold-formed steel section length for specimens (MWS3-1 and MWS3-2), force the model to fail with initiation of flexure cracks, ended with brittle shear failure, as shown in Figs. 11(a-b). While specimen (MWS3-3) with three-web cold-formed steel section and full length, failed due to web local buckling. The concrete cracks initiation delayed by (22, 17, and 10%) for models (MWS3-1, MWS3-2 and MWS3-3), respectively.

(a) MWS3-1

(b) MWS3-2

(c) MWS3-3

Fig. 11. Failure mode for models (group C).

Specimens (MWS3-1 and MWS3-2) fail before the cold-formed section reach yield, due to the model brittle shear failure. Increasing by (80 and 35%) (In average) in the mid-span strain for a specimen (MWS3-3, MWS3-2 respectively), with respect to specimen (MWS3-1) was observed, Fig. 12.

In aim of declare the relationship between the failure load and cracking load, cracking factor (F_{cr}), was introduced as the percentage of the load at which first concrete crack initiated to the failure load. The cracking factor for the reference beam was 66%.

For the first group this factor was approximately the same as the reference beam for models (MWS1-2, MWS1-3), and was reduced to (59%) for model (MWS1-6) which provided good announcing before failure, while this factor increased to (76 ,76 and 71%) for models (MWS1-1 , MWS1-4 and MWS1-5) respectively as shown in Fig. 13(a). The cracking factor increased for the second group to 78% in average for models (MWS2-1, MWS2-2, MWS2-3 and MWS2-4) respectively, as shown in Fig. 13(b). The cracking factor for the third group was approximately the same as the reference beam for models (MWS3-1, MWS3-2), increased to 76% for model MWS3-3, Fig. 13(c).
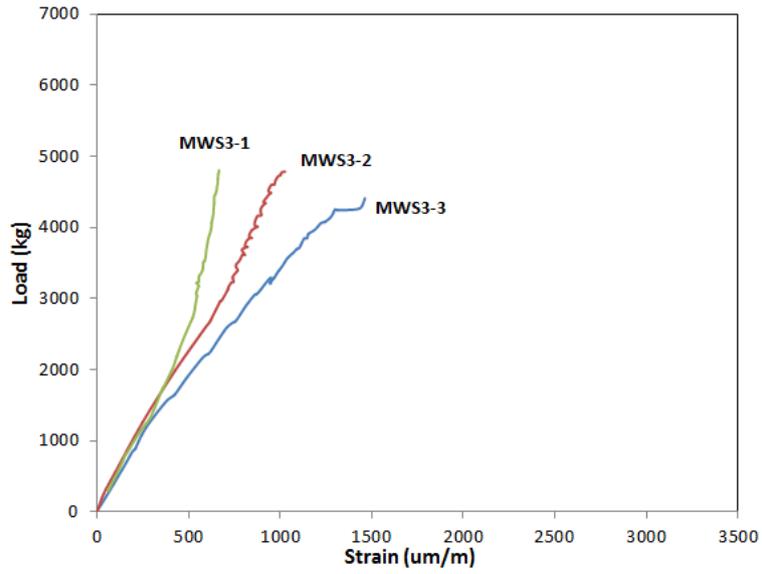
Fig. 12. Mid-span strain (Group C).
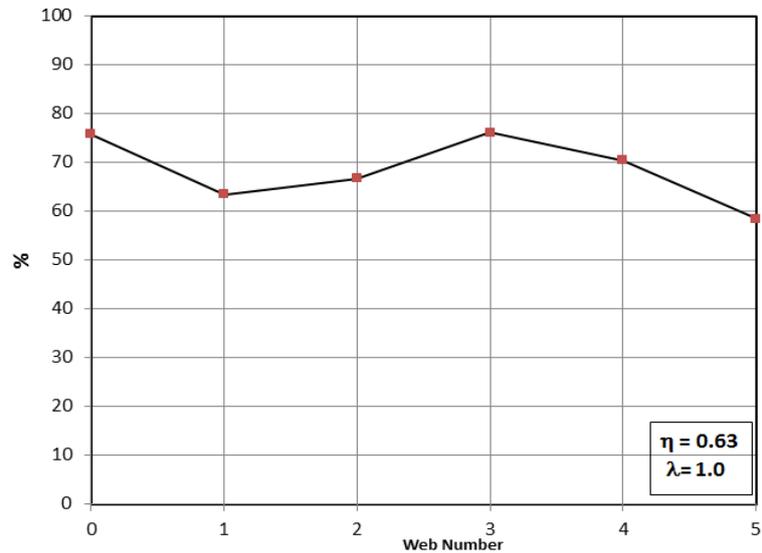
(a) Group A
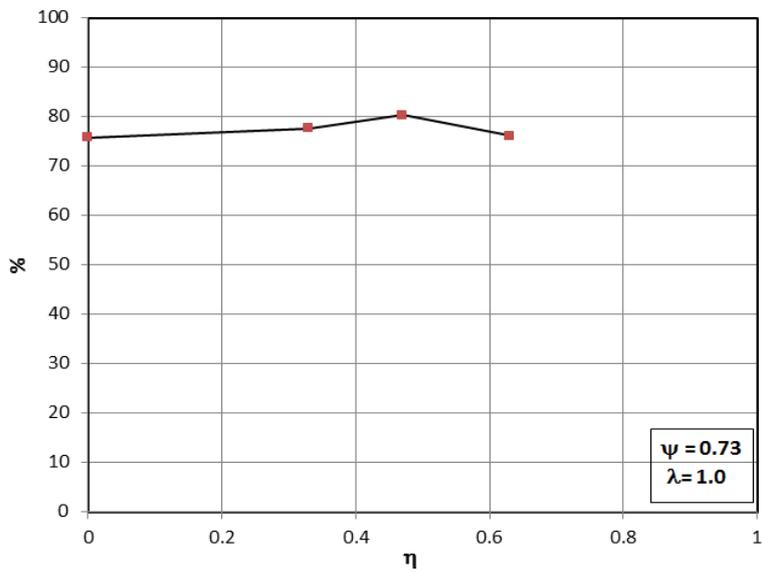
(b) Group B

Fig. 13. (continued)
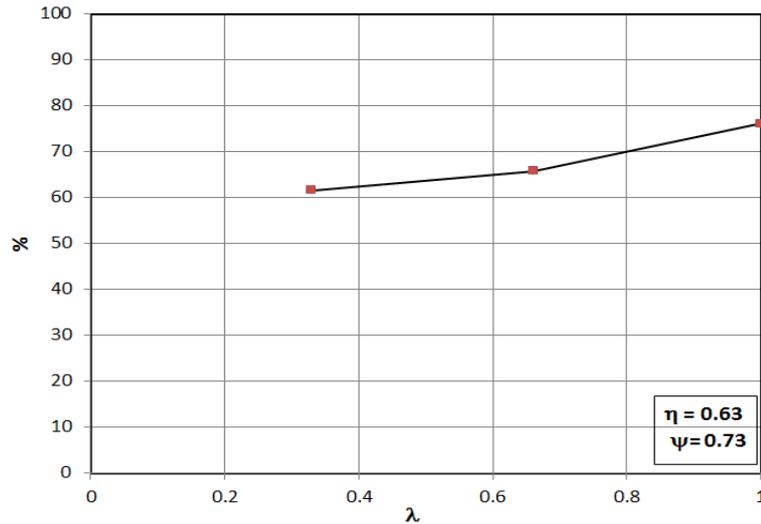
(c) Group C

Fig. 13. Cracking factor.

4.2. Deflections

The deflection-load curves for models with one-center web (MWS1-2) and that with five webs (MWS1-6) at the beam mid-span (dial 3), were plotted, and compared with that of the reference beam. The curves illustrate the ductile (flexure) failure for both reference beam and model with one-center web, while increasing the number of webs to five changes the mode of failure to brittle failure. The curves also indicate that increasing the number of webs to five decreases the deflection by about 35% (in average) with respect to reference beam, as shown in Fig. 14(a). Fig. 14(b) represents the deflection-load curves for group A, the figure indicates decrease in deflection by 33% in average for models with 3, 4 and 5 webs with respect to reference beam.

Fig. 14(c) represents the deflection-load curves for group B, the figure indicates decrease in deflection by 40% in average for model (MWS2-4), with no noticeable change for other models.

Using of the three-web cold-formed section with total length, two-third, and one-third the concrete beam length

decreases the deflections by average values of 33, 30, 5% respectively with respect to reference beam, Fig. 14(d).

In addition, the deflected shapes for specimens (MWS1-2, MWS1-6), along the beam length were plotted at a certain load level (linear stage), and was compared with the deflected reference beam, as shown in Fig. 15(a). The figure shows that there was a decrease of (7, 23% in average), in the beam deflection for specimens (MWS1-2, MWS1-6) respectively, with respect to that of reference beam. From that, the Multi-web sections shared in decreasing the deflections more than that of reference beam.

The deflected shapes for specimens (MWS3-1, MWS3-3) were plotted along the beam length at the same load level (linear stage), and was compared with that of reference beam, as shown in Fig. 15(b). The figure shows that there was a decrease of (8, 38% in average), in the beam deflections for specimens (MWS3-1, MWS3-3) respectively, with respect to that of reference beam. From that, the full-length cold-formed steel section shared in decreasing the deflections more than that with less length.
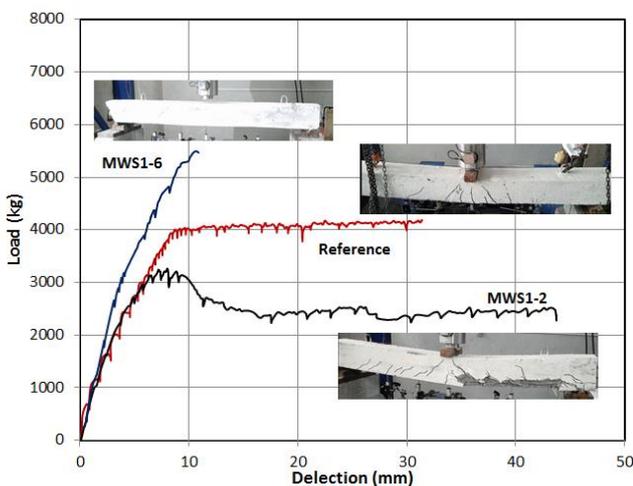
(a) MWS1-2, MWS1-6
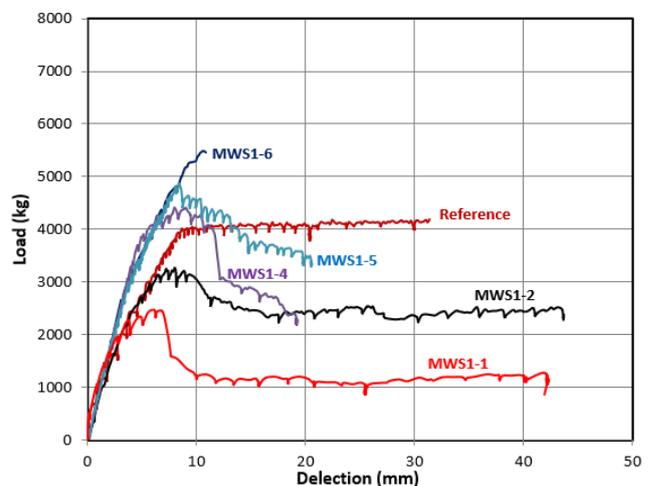
(b) Group A

Fig. 14. (continued)

(c) Group B   (d) Group C

Fig. 14. Deflection-load curves.

(a) MWS1-2, MWS1-6

(b) MWS3-1, MWS3-3
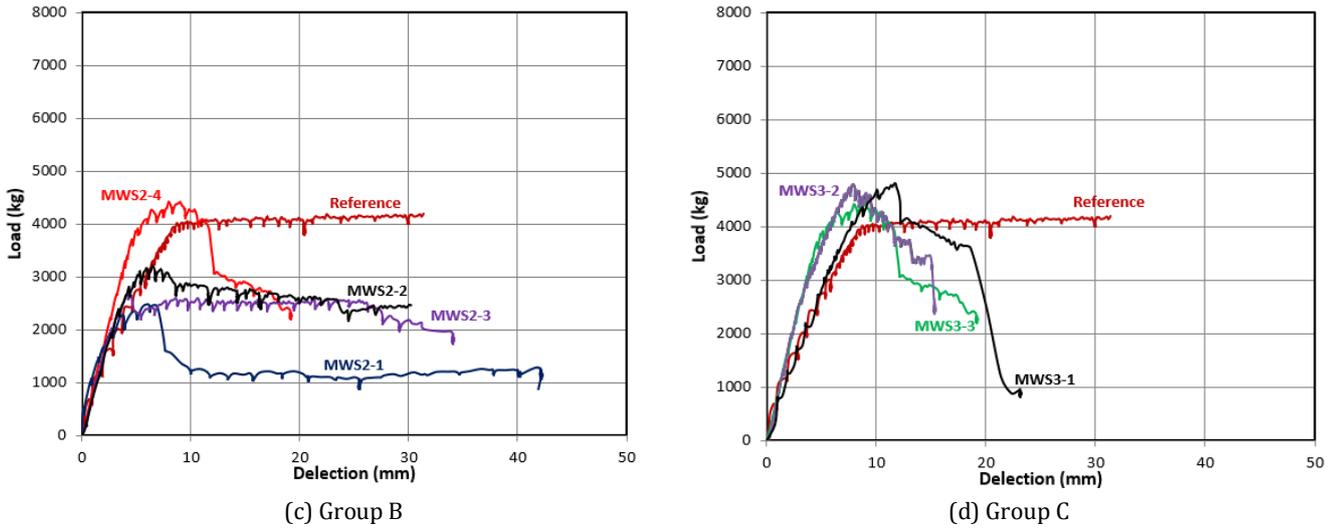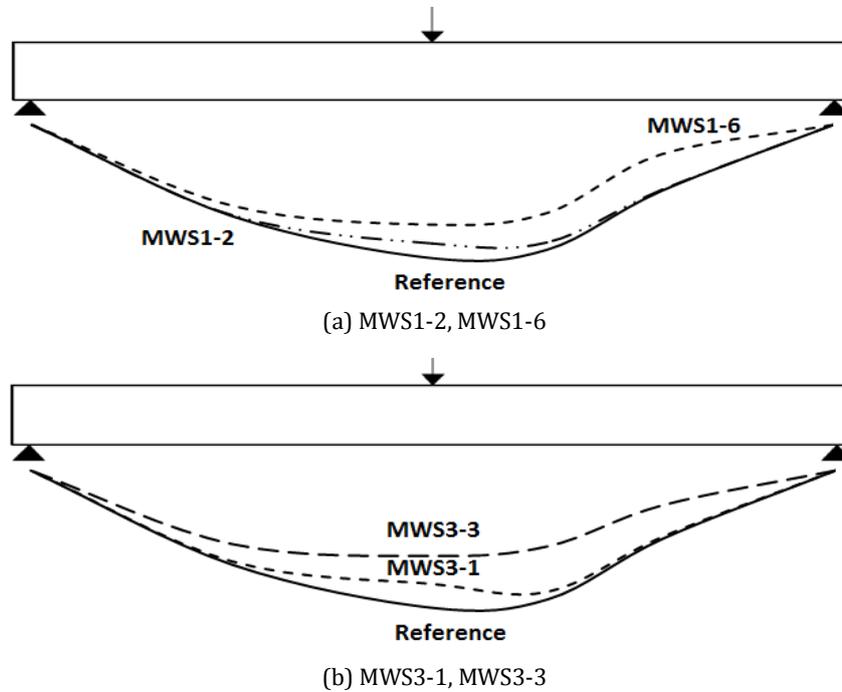
Fig. 15. Deflected shapes.

4.3. Factor of ductility

By applying the fracture mechanics concepts, there could be a safety margin against failure with reasonable reliability, also a safety margin for prediction the beam failure. Factor of Ductility (F_d) is defined as the ratio of mid-span deflection at beam failure to that at the first concrete crack, the reference beam factor of ductility was 6.5, as shown in Table 2.

Figs. 16(a-c) shows (F_d) variation with the web (number, height, and length) respectively. It declared that the ductility factor decreased as the web number and normalized height increased, while variation of the normalized length had no noticeable effect on the factor of ductility (all were less than that of reference beam). The ductility factor was observed to be the highest for models (MWS1-1 and MWS1-1), then the reference beam.

5. Conclusions

Through the experimental research on the multi-web cold-formed steel section structural behavior, the following conclusions were obtained:
- Providing a multi-web cold-formed steel section increase the beam load capacity with a significant value and make good benefits of using cold-formed steel section.
- Providing a multi-web cold-formed steel section decrease the beam deflection with a significant value.
- Increasing the number of webs for the cold-formed steel section has a significant effect in decreasing the stress on the cold-formed steel section.
- Shear splitting failure can be avoided by using end web sections.
- Local buckling in the cold-formed steel governs the structural element failure.

- Reducing the multi-web cold-formed steel section length (less than two-thirds of beam length), increase the beam load capacity with a significant value, than using full length, but led to brittle shear failure.

- Reducing the multi-web cold-formed steel section length (two-thirds of beam length), decrease the beam deflections approximate the same of that with full-length with a significant value.

(a) Group A

(b) Group B

(c) Group C
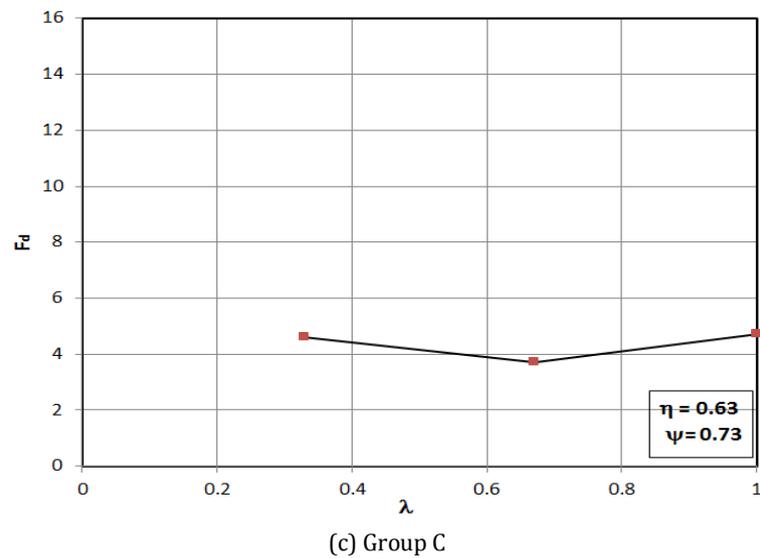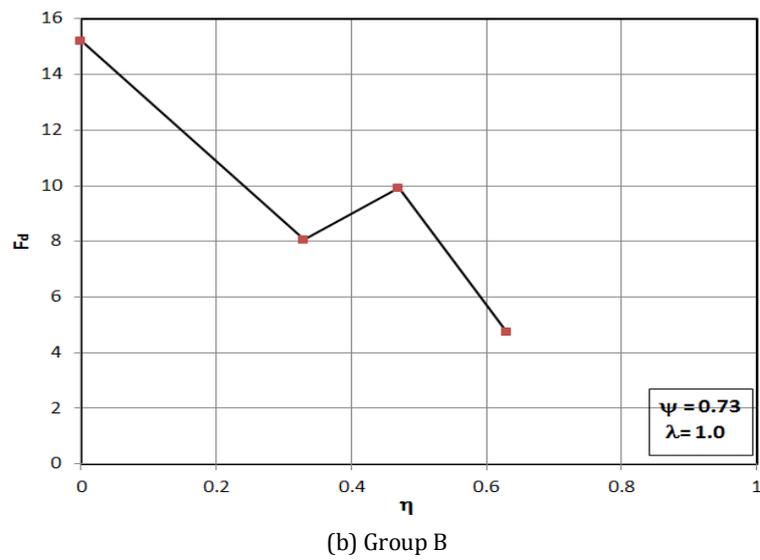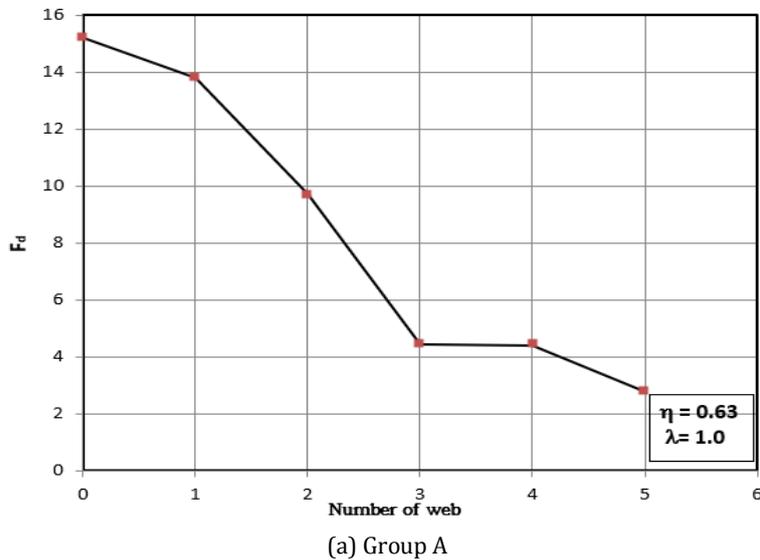
Fig. 16. Factor of ductility.

REFERENCES

Ammar A, Saad N, Wael S (2012). Strength and ductility of concrete encased composite beams. *Engineering and Technology Journal*, 30, 2701-2714.

Bedair O (2015). Design expression for web shear buckling of box sections by accounting for flange restraints. *Journal of Constructional Steel Research*, 110, 163–169.

CEN, Eurocode 3 (2005). Design of Steel Structures, Part1-3: General Rules — Supplementary Rules for Cold-formed Steel Members and Sheeting. European Committee for Standardization, Brussels.

Gilbert BP, Savoyat TJM, Teh LH (2012b). Self-shape optimisation application: optimisation of cold-formed steel columns. *Thin-Walled Structures*, 60, 173–184.

Gilbert BP, Teh LH, Guan H (2012a). Self-shape optimization principles: optimization of section capacity for thin-walled profiles. *Thin-Walled Structures*, 60, 194–204.

Hancock GJ (2007). Design of Cold-formed Steel Structures, 4th Edition. Australian Steel Institute, North Sydney, Australia.

Lanc D, Vo TP, Turkalj G, Lee J (2015). Buckling analysis of thin-walled functionally graded sandwich box beams. *Thin-Walled Structures*, 86, 148-156.

Leng J, Guest JK, Schafer BW (2011). Shape optimization of cold-formed steel columns. *Thin-Walled Structures*, 49, 1492–1503.

Liu H, Igusa T, Schafer B (2004). Knowledge-based global optimisation of cold-formed steel columns. *Thin-Walled Structures*, 42, 785–801.

Ma W, Becque J, Hajirasouliha I, Ye J (2015). Cross-sectional optimization of cold-formed steel channels to Eurocode 3. *Engineering Structures*, 101, 641 - 651. ISSN 0141-0296

Madeira JFA, Dias J, Silvestre N (2015). Multi-objective optimisation of cold-formed steel columns. *Thin-Walled Structures*, 96, 29–38.

Moharrami M, Louhghalam A, Tootkaboni M (2014). Optimal folding of cold-formed steel cross sections under compression. *Thin-Walled Structures*, 76, 145–156.

Pham SH, Pham CH, Hancock GJ (2014). Direct strength method of design for shear including sections with longitudinal web stiffeners. *Thin-Walled Structures*, 81, 19-28.

SFIA (2012), Technical Guide for Cold-Formed Steel Framing Products. Steel Framing Industry Association, United States of America.

Wang B, Bosco GL, Gilbert BP, Guan H, Teh LH (2016). Unconstrained shape optimisation of singly-symmetric and open cold-formed steel beams and beam columns. *Thin-Walled Structures*, 104 54–61.

Ye J, Hajirasouliha I, Becque J, Pilakoutas K, (2016). Development of more efficient cold-formed steel channel sections in bending. *Thin-Walled Structures*, 101, 1-13.

Yu WW (2010). Cold-Formed Steel Design, 4th Edition. Wiley, Hoboken, United States of America, NJ.